AN EXPERIMENTAL AND NUMERICAL INVESTIGATION TO ENHANCE HEAT TRANSFER IN POROUS HEAT EXCHANGERS FOR WASTE HEAT RECOVERY SYSTEM

Mahesh K[1*] and Jayaraman B[2]

[1*] Department of Mechanical Engineering, Srinivasa Ramanujan Centre, SASTRA Deemed University, Kumbakonam – 612001, Thanjavur, Tamil Nadu, India.

[2] Department of Mechanical Engineering, SASTRA Deemed University, Thanjavur – 613401, Tamil Nadu, India.

[*] Corresponding author; E-mail: machbala@src.sastra.edu

The energy from an IC engine's exhaust gas can be used to operate a vapour absorption refrigeration system, which cools the interior of the vehicle. An exhaust gas-powered porous heat exchanger can be used in place of a generator in vapour absorption refrigeration systems. In this study, a double pipe counter flow heat exchanger with and without porous materials (wire screens) is analyzed numerically to maximise heat transfer from hot air to cold fluid with a minimum of pressure drop using the Ansys Fluent tool. Wire screens are used in this heat exchanger due to their higher surface area density. In order to assess their effects on the heat exchanger's effectiveness, the number transfer unit, and the pressure drop under steady-state conditions, tests are conducted. The impacts of the wire screens presence are investigated for both water and aqua ammonia as cold fluids, as well as for varying hot air mass flow rates. Furthermore, the numerical estimations of heat transfer from hot air to cold water are validated by experimental data. Compared to a heat exchanger without porous material, the effectiveness of a porous heat exchanger increases from 0.17 to 0.33. The numerical investigation outcomes and the experimental validation are quite comparable.

Key words: *Porous Media Heat exchanger, Wire screens, Computational fluid dynamics, Vapour Absorption Refrigeration*

1. Introduction

The use of porous media to improve heat transfer rates has seen a remarkable increase in research over the last two decades. Enhancing the rate of heat and mass transport in energy systems through the use of porous media has many benefits. Heat exchangers with porous media provide a considerable heat transfer capacity in a compact design. The potential of metal-based porous media to promote heat transmission, which benefits the operation of various heat exchangers, has been extensively explored. Wire screens are employed in regenerators due to the greater area of their surface density.

E. Brundrett [1] investigated the pressure loss correlation by studying flow through metallic wire screens with Reynolds numbers ranging from 10^{-4} to $l0^{4}$ utilizing conventional orthogonal porosity and a function of wire Reynolds number. Bogdan I. Pavel and Abdulmajeed A. Mohamad [2] examined the impact of metallic porous materials placed in a pipe on the rate of heat transfer and pressure drop by

measuring the porosity effects, diameter, thermal conductivity and the Reynolds number. Chen Shuangtao et al. [3] studied a numerical model of a wire screen heat exchanger that was created and validated under certain conditions using the ε-NTU technique. J.P. Yadav and Bharat Raj Singh [4] analysed the availability of heat in hot exhaust emitted by car engines, a vapour absorption refrigeration system is a highly effective method for providing a refrigerating effect in automobiles. Wael I.A. Aly et al. [5] report that waste heat from diesel engine exhaust gas was utilised as an energy source to evaluate a diffusion absorption refrigerator's thermal performance. The internal flow properties of sintered metal wire screen structures with different porosities were studied by Y B Peng et al. [6]. Edgar Avalos Gauna and Yuyuan Zhao [7] examined heat transfer and fluid flow in open-cell porous metals developed via space holder techniques using numerical modeling. Isbeyeh W. Maid et al. [8] examined the improvement of heat transfer in a double pipe counter flow heat exchanger with an inner tube metallic pad insert. As the heat transfer surface, Hannes Fugmann et al. [9] examined a variety of test pieces of heat exchangers with various wire configurations. Nikolai Chernov [10] developed a technique that entails finning a macrorelief with optimal geometric properties in order to increase the area of heat exchange surfaces in contact with heat carriers. Patrick N. Okolo et al. [11] studied the properties of low turbulence fluid flow over woven wire screens using two different types of computational grids. An appropriate turbulence model for woven wire screens and their related applications has been discovered, which offers loss coefficients within 1% to 8% of experimental values. A model of a porous regenerator Stirling cryocooler was designed, developed, and manufactured by K.V. Srinivasan et al. [12] using the additive manufacturing process of Direct Metal Laser Sintering.

Mukul Kumar and Randip Kumar Das's [13] research suggests that the generator for the refrigeration system may be placed directly in the path of exhaust fumes. This would allow the system to operate entirely on the waste energy from these gasses without the need for an electric heater. J. Siddhartha Yadav et al. [14] attempted to tackle this problem by developing a vapour absorption system that used waste heat technology to produce the necessary refrigerating effect for a 1.5 TR air conditioner. The efficiency of a single row water-to-air cross flow heat exchanger in terms of heat transfer and pressure drop was assessed by M.A. Sayed et al. [15]. Ten copper pipes that are placed uniformly make up the heat exchanger. Salem Alabd Mohamed and Munawar Nawab Karimi [16] explored how changing the baffle spacing of a generator heat exchanger operating on a single effect LiBr /water absorption cycle could improve heat transfer. Isbeyeh W. Maid et al. [17] developed a numerical simulation to examine heat transmission in a double tube heat exchanger with and without porous material. Xiang-Bo Feng et al. [18] investigated convective heat transfer in porous media using the cascaded lattice Boltzmann method at the representative elementary volume scale. Andr'es Zapata et al. [19] designed a CFD bubble absorber model that was used for modelling the absorption process in a tubular absorber utilising an NH3/LiNO3 solution.

Trilok G et al. [20] investigated on the relationships between the morphological features of packed wire screens, which depend on the mesh size, wire diameter, and stack type. These correlations are crucial for defining the medium's properties and locating crucial input variables needed for computational modelling. Le Xuan Hoang Khoa et al. [21] developed a computer algorithm to examine the effects of fin length, number, location, and structure (solid or porous) on heat transfer and the flow field in a differentially heated chamber with solid or porous fins. O.H. Hassan et al. [22] examined the forced convection heat transfer characteristics of turbulent flow that generate internal heat and the pressure drop across the channel in a cylindrical channel filled with porous material. Saad S. Alrwashdeh

et al. [23] studied the impact of heat exchanger length on parallel and counter flow heat exchangers using computational simulation tools. The impact of heat and mass transfer on mixed convection fluid movement via a horizontal channel was examined by Ghanim M. Algwauish et al. [24]. Eman Mohamed Ismail et al. [25] investigated the thermal performance of various inserts and tubes in heat exchangers and found that distinct thermal enhancement factors are found when comparing plain tapes, plain tubes, and customized inserts. Zengliang Chen et al. [26] studied the most effective way to design and operate the heat exchanger in the oil and gas recovery system at the oil depot. Jiangtao Chen et al. [27] evaluated the prediction model and parameter optimization by analyzing engineering data from an absorption heat exchanger with a large temperature difference. In this study, metallic wire screens were inserted within the annular pipe to enhance heat transmission in counter flow heat exchangers. The performance of the heat exchanger is compared with experimental findings using numerical simulation.

2. Theoretical background

2.1. Waste heat recovered refrigeration system

The vapour compression refrigeration technique is the most prevalent mechanism utilised in automotive air conditioning. A vapour absorption refrigeration system is employed to provide a refrigerating effect. A vapour absorption refrigeration system replaces the compressor with a regenerative heat exchanger or generator, a pump, and an absorber. In a vapour absorption refrigeration system with ammonia as a refrigerant and water as an absorbent is employed, which is a very profitable choice to generate a refrigerating effect in automobiles due to the existence of heat in hot exhaust coming from automotive engines. In order to investigate waste heat recovery technology, this study looks at a porous heat exchanger that is filled with wire screens for a vapour absorption refrigeration system.

2.2. Porous heat exchanger

Wire screens are a preferred material for heat exchange in porous heat exchangers because of their higher surface area density. The wire screen packed heat exchanger is shown in fig. 1a. This study emphasises on the operation of these stacked wire screens in heat exchangers, and validates the wire screen's airflow resistance and heat transfer rate through numerical analysis and experiments. Fig. 1b shows some varieties of porous wire screens (meshes).

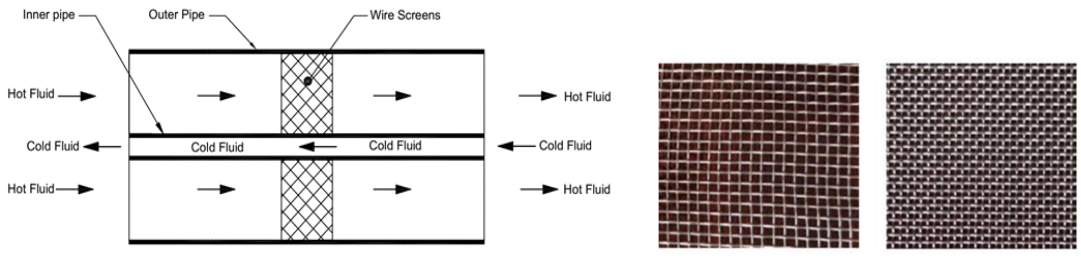

(a) (b)

Figure 1. (a) Porous counterflow heat exchanger, (b) Porous wire screens

2.3. Numerical setup

The numerical simulations of the double pipe counter flow heat exchanger with wire screens is carried out in order to minimize pressure loss and maximize the rate of heat transfer. In the middle of

the heat exchanger's outer pipe are 35 layers of wire screens with a porosity of 0.64. The effects of the wire screens are investigated for various hot air mass flow rates using aqua ammonia and water as cold fluids. In the numerical simulations, a 20 % aqua ammonia solution with a density of 0.92 g/mL, thermal conductivity of 0.45-0.48 W/(m·K) at 25 °C and viscosity of 1.1-1.3 mPa·s at 25 °C are taken into consideration. An analysis is conducted on the numerical estimates of heat transfer from hot air to cool aqua ammonia. The hot air is transmitted into the outer tube through the metallic wire screens, while cold aqua ammonia is transferred in the opposite direction into the inner tube. Furthermore, the numerical estimations of heat transfer from hot air to cold water are validated by experimental data. The purpose of this work is to better understand the flow characteristics via wire screens by using CFD based simulations of fluid flow using ANSYS FLUENT. Fig. 2, illustrates the three zones of the model. The porous zone, which is packed with wire screens, is located in the center of the outer pipe. An inner pipe transfers the cold fluid, and an outer pipe transfer the hot fluid in this annular pipe flow.

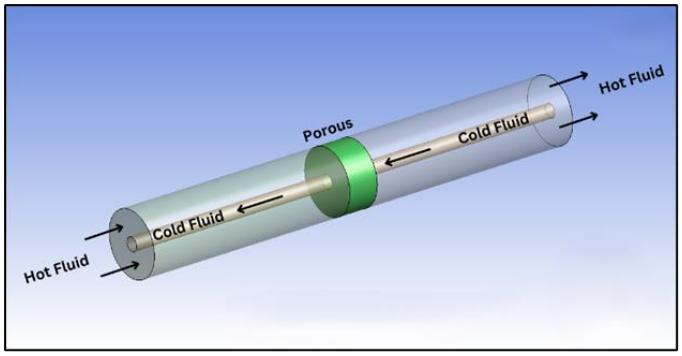

Figure 2. Porous Counter Flow Heat exchanger

2.4. Governing equations

The continuity equation is used to solve the Navier-Stokes and thermal energy transfer equations numerically for Newtonian fluids:

$$\frac{\partial(\varepsilon\rho)}{\partial t}+\nabla.\left(\varepsilon\rho\vec{v}\right)=0 \tag{1}$$

The basic fluid-flow equations are extended to include a momentum source term, Si, to characterise the porous medium. According to Equation (2), the original term is separated into an inertial loss term and a viscous loss term.

$$\frac{\partial(\varepsilon\rho\vec{v})}{\partial t}+\nabla.(\varepsilon\rho\vec{v}\vec{v})=-\varepsilon\nabla p+S_i \tag{2}$$

The momentum source component is added to the fundamental fluid flow equations to reflect flows through perforated sheets, packed beds, tubular banks, and filter materials. Both an inertial and a viscous loss term forms the source term.

$$S_i=-\left(\sum_{j=1}^{3}D_{ij}\mu v_j+\sum_{j=1}^{3}C_{ij}\frac{1}{2}pv_{mag}v_j\right) \tag{3}$$

The source term of the ith x, y, or z momentum equation is Si, and the indicated matrices are D and C. Using a basic homogeneous porous material, as follows:

$$S_i=-\left(\frac{\mu}{K}v_i+C_2\frac{1}{2}\rho|v|v_i\right) \tag{4}$$

where the inertial resistance factor, C2, and the permeability, K, are computed as follows:

$$K = \left(\frac{\varepsilon^3 d^2}{150(1-\varepsilon)^2} \right) \tag{5}$$

$$C_2 = \frac{3.5}{d} \frac{(1-\varepsilon)}{\varepsilon^3} \tag{6}$$

Energy equation

The governing energy equation for porous media often include a heat transfer term between the fluid and solid phases as well as a heat conduction term based on the effective thermal conductivity of the porous medium.

$$\left(\rho c_p\right)^* \frac{\partial T}{\partial t} + \left(\rho c_p\right)_f \varepsilon \vec{v}.\nabla T = \left(\rho c_p\right)_f \alpha_{eff} \nabla^2 T \tag{7}$$

$$\left(\rho c_p\right)^* = \varepsilon \left(\rho c_p\right)_f + (1-\varepsilon)\left(\rho c_p\right)_s \tag{8}$$

Effective conductivity in a porous medium:

$$k_{eff} = \varepsilon k_f + (1-\varepsilon) k_s \tag{9}$$

where k_f and k_s, stand for the thermal conductivities of fluids and solids, respectively.

2.5. Heat exchanger analysis

In order to analyse a heat exchanger, numerous crucial assumptions must be made. Thus, it is assumed that the flow characteristics are as follows:

- Incompressible fluid and steady state conditions.
- Fluids do not undergo phase changes.
- The consequences of radiation heat transfer are disregarded.
- Heat transmission between the cold and hot fluids alone, with perfect heat exchanger insulation.
- The physical characteristics of both the solid and fluid phases stay unchanged throughout the operation.

The heat dissipation of both fluid sides are:

$$Q_c = m_c C_{pc} \left(T_{co} - T_{ci}\right) \tag{10}$$

$$Q_h = m_h C_{ph} \left(T_{hi} - T_{ho}\right) \tag{11}$$

An estimate of the overall heat transfer coefficient, or U, can be obtained from:

$$Q_{act} = U_i A_i LMTD \tag{12}$$

$$U = \frac{Q_{act}}{A_i * LMTD} \tag{13}$$

The log mean temperature difference between the hot and cold fluids can be obtained from:

$$LMTD = \frac{\Delta T_1 - \Delta T_2}{In\left(\frac{\Delta T_1}{\Delta T_2}\right)} \tag{14}$$

$$\Delta T_1 = \left(T_{hi} - T_{co}\right) \; \Delta T_2 = \left(T_{ho} - T_{ci}\right) \tag{15}$$

Maximum possible heat transfer, Q max, effectiveness, ε, and number of transfer unit, NTU, and C_r from the following relations:

$$Q_{\max} = C_{\min}\left(T_{hi} - T_{ci}\right) \tag{16}$$

$$\in = \frac{Q_{act}}{Q_{\max}} \tag{17}$$

$$NTU = \frac{UA_i}{C_{\min}} \tag{18}$$

Capacity ratio

An exchanger's capacity ratio (C_r) is a dimensionless number that shows the proportion of the two fluids' smaller heat capacity rates to their larger heat capacity rates.

$$C_r = \frac{C_{\min}}{C_{\max}} \tag{19}$$

3. Experimental apparatus

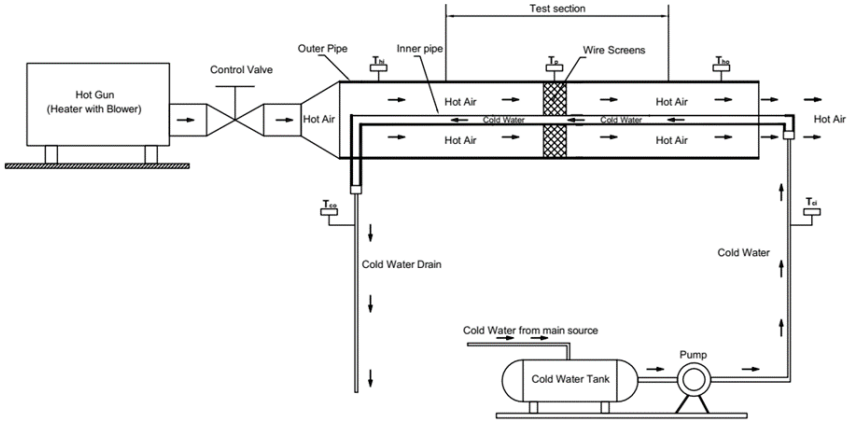

Figure 3. Illustration showing the experimental setup and test portion.

An arrangement for the experiment structure and test section details are shown in fig. 3.The test heat exchanger comprises of the wire screens (Porous media) in the outer pipe of the counterflow heat exchanger, a blower with a heater that feeds hot air through the test section, control valve that regulates the air velocity, the cold water tank that maintains the water level from the main supply, the feed water pump that supply the cold water in the inner pipe of heat exchanger, and digital LED display temperature sensors that monitor the temperature of hot and cold fluids at the inlet and outlet of porous heat exchanger. The hot blower and feed water pump are powered by an AC source. Fig. 4 shows a photograph of the counterflow heat exchanger's rig assembly. The steel double cylindrical concentric pipes in the test section have a length of 915 mm, an inner pipe diameter of 19 mm, and an outer pipe diameter of 75 mm, with wall thickness of 1mm and 3 mm respectively. Thermal insulation was provided by a 25 mm-thick sheet of glass wool placed in the test area to prevent heat loss.

Figure 4. Photograph of rig assembly

4. Results and discussion

4.1. Numerical results

The heat exchanger's performance was examined by altering the hot air mass flow rates in the outside pipe with wire screens while maintaining constant mass flow rates of cold aqua ammonia flowing inside the inner pipe. The heat exchanger was numerically evaluated using its 535 mm length, 75 mm outer pipe diameter, 16 mm inner pipe diameter, and 35 layers of wire screens located in the center of the outer pipe. The heat exchanger's temperature distribution utilizing porous materials at hot air and cold aqua ammonia mass flow rates of 0.010 and 0.02 kg/s, respectively, is shown in fig. 5a.

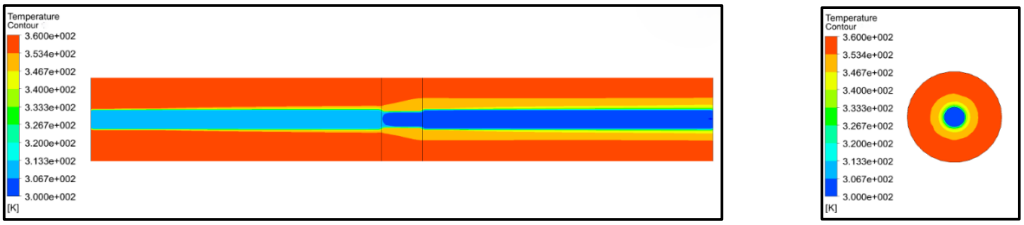

Figure 5-a. Temperature distribution with porous and mass flow rates (0.010, 0.02 kg/s) for hot air and cold aqua ammonia

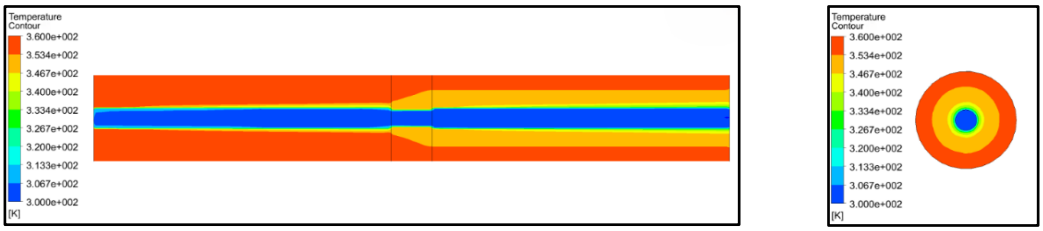

Figure 5-b. Temperature distribution with porous, and mass flow rates (0.006, 0.02 kg/s) for hot air and cold aqua ammonia

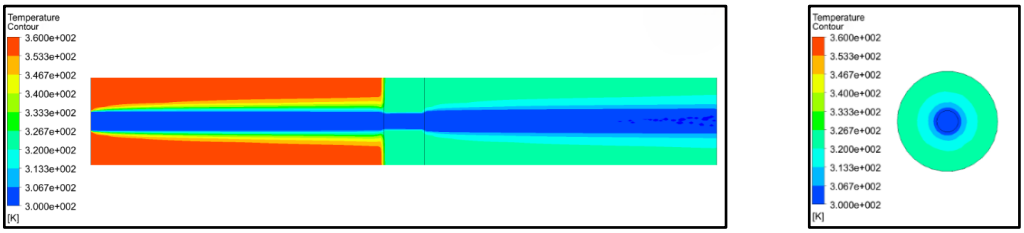

Figure 5-c. Temperature distribution with porous, and mass flow rates (0.0005, 0.02 kg/s) for hot air and cold aqua ammonia

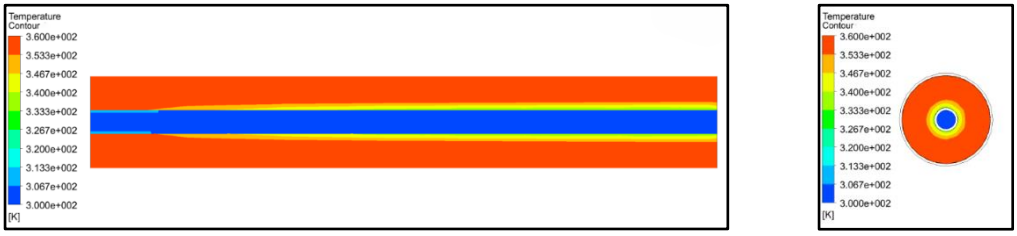

Figure 5-d. Temperature distribution without porous and mass flow rates (0.010, 0.02 kg/s) for hot air and cold aqua ammonia

Based on the findings of the simulations of the cold inlet aqua ammonia solution at 27 °C and the hot air intake at 87 °C that crossed the porous medium, the cold aqua ammonia outlet temperature increased by 9.43 °C with a heat transfer rate of 109.6 w/m^{2}K. Fig. 5b illustrates the temperature distribution in the presence of porous materials. The mass flow rate for hot air is reduced to 0.006 kg/s, while the cold aqua ammonia flow rate remains constant at 0.02 kg/s. At a heat transfer rate of 78.8 w/m^{2}K, the temperature of the cold aqua ammonia outflow increased by 6.78 °C. It is obvious from this that a higher in mass flow rate will result in a rise in temperature and the rate of heat transfer. Fig. 5c illustrates how the hot air in the outer pipe crosses the porous section. Because of the hot air's low mass flow rate and inability to transfer heat energy to cold aqua ammonia, the hot air temperature is lowered.

The heat exchanger without porous materials was simulated for the mass flow rates of hot air at 0.010 and cold aqua ammonia at 0.02 kg/s, respectively, as shown in fig. 5d. When comparing a heat exchanger with and without porous material, the one with porous material has the maximum thermal energy transmission (fig. 5a & fig. 5d). Furthermore, in a numerical simulation, water was used as the cold working fluid instead of aqua ammonia. As the mass flow rate of hot air is 0.010 kg/s, fig. 6a, illustrates a 6.05 °C increase in the cold water outlet temperature and a 91.07 W heat transfer rate. This rise is based on the hot air intake at 87 °C and the cold input water at 27 °C that passed the porous medium.

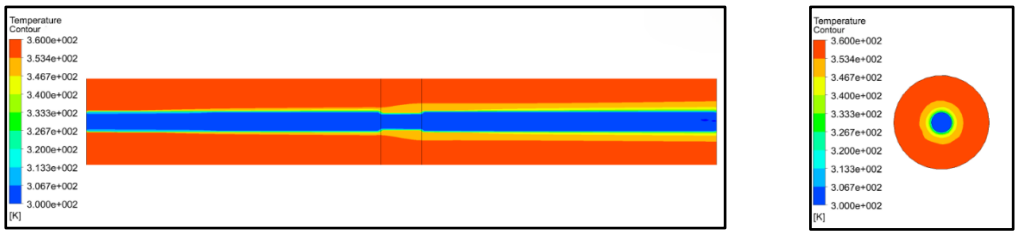

Figure 6-a. Temperature distribution with porous and mass flow rates (0.010, 0.02 kg/s) for hot air and cold water

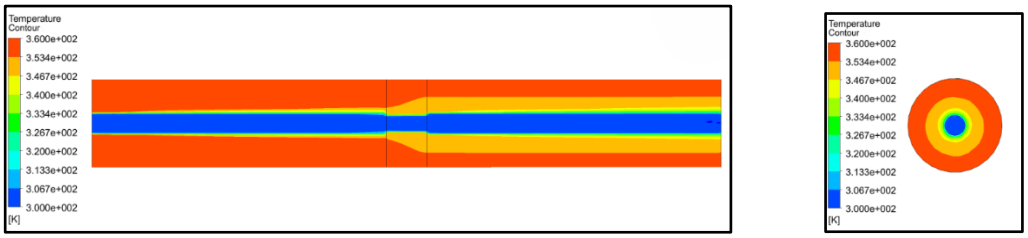

Figure 6-b. Temperature distribution with porous, and mass flow rates(0.006, 0.02 kg/s) for hot air and cold water

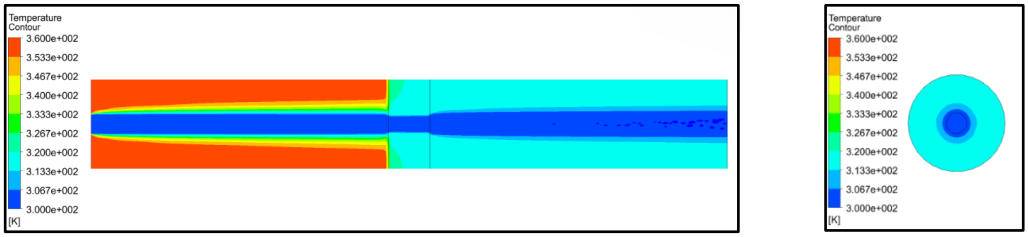

Figure 6-c. Temperature distribution with porous, and mass flow rates (0.0005, 0.02 kg/s) for hot air and cold water

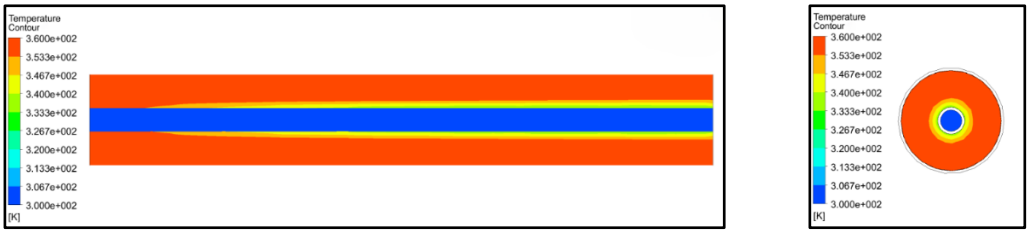

Figure 6-d. Temperature distribution without porous and mass flow rates (0.010, 0.02 kg/s) for hot air and cold water

Fig. 6b, displays the temperature distribution of a heat exchanger with porous materials. The simulation's outcome indicated that heat transfer was reduced to 76.96 W due to a drop in the mass flow rate of hot air. The flow of hot air across the porous section of the outer pipe is shown in fig. 6c. As seen in fig. 6d, the heat exchanger without porous materials is simulated for the mass flow rates of cold water at 0.02 kg/s and hot air at 0.010 kg/s, the cold water outlet temperature increases to 3.14 °C and a heat transfer rate is 34.98 W. A heat exchanger with porous material has the maximum heat transfer as compared to one without porous.

4.2. Experimental validation

The counter flow heat exchanger without porous screens' estimated NTU and effectiveness are displayed in tab. 1. Similarly, tab. 2 displays the calculated NTU and effectiveness of the porous screens counterflow heat exchanger. The findings indicate that an increase in mass flow rate and hot air intake temperature will result in a rise in NTU and effectiveness. In comparison to a heat exchanger without porous material, the effectiveness of a porous heat exchanger increases from 0.17 to 0.33 (tab.1 and tab.2). In both cases (WP and WOP), effectiveness rises in parallel with NTU.

Table 1. Effectiveness and NTU calculated for the counterflow heat exchanger without porous materials (WOP)

Sl.No.	Mass flow rate of hot air $\dot{m}$ (kg/s)	Actual heat transfer rate Q_{act} (kJ/s)	Maximum heat transfer rate Q_{Max} (kJ/s)	Effectiveness ϵ	NTU
1	0.006	0.028	0.253	0.111	0.148
2	0.006	0.041	0.339	0.120	0.157
3	0.006	0.054	0.401	0.134	0.161
4	0.010	0.063	0.434	0.148	0.184
5	0.010	0.089	0.571	0.157	0.192
6	0.010	0.115	0.672	0.171	0.198

Table 2. Effectiveness and NTU calculated for the counterflow heat exchanger with porous materials (WP)

Sl.No.	Mass flow rate of hot air $\dot{m}$ (kg/s)	Actual heat transfer rate Q_{act} (kJ/s)	Maximum heat transfer rate Q_{max} (kJ/s)	Effectiveness ϵ	NTU
1	0.006	0.041	0.259	0.158	0.190
2	0.006	0.058	0.350	0.168	0.208
3	0.006	0.079	0.408	0.194	0.224
4	0.010	0.115	0.441	0.261	0.299
5	0.010	0.174	0.578	0.302	0.346
6	0.010	0.226	0.679	0.332	0.372

The experimental observations of the counter flow heat exchanger without porous materials are shown in tab. 3. The hot air outlet temperatures in the heat exchanger's outer pipe are collected by varying the hot air input temperatures and hot air mass flow rates. Furthermore, the temperatures of the cold water outflow were collected in the heat exchanger's inner pipe in the opposite direction at a fixed cold water mass flow rate and constant inlet temperature. Similarly, tab. 4 presents the experimental results of the heat exchanger with porous material. The experimental findings clearly demonstrate that increased heat transfer is caused by rising hot air mass flow rates as well as rising hot air input temperatures. It is also clear that a heat exchanger with porous material has a cold water exit temperature that is higher than one without porous material (tab. 3 and tab. 4).

Table 3. Measurements obtained from the counterflow heat exchanger without porous screens (WOP)

Sl.No.	Mass flow rate of hot air ṁ (kg/s)	Hot air inlet temperature T (°C)	Hot air outlet temperature T(°C)	Cold water inlet temperature T (°C)	Cold water outlet temperature T (°C)
1	0.010	87.4	79.6	27	31.7
2	0.010	84.5	67.2	27	31.1
3	0.010	71.2	56.9	27	30.5
4	0.006	87	75.5	27	31.1
5	0.006	84	61.5	27	30.6
6	0.006	70.1	52.2	27	30.1

Table 4. Measurements obtained from the counterflow heat exchanger with porous screens (WP)

Sl.No.	Mass flow rate of hot air ṁ (kg/s)	Hot air inlet temperature T(°C)	Hot air outlet temperature T (°C)	Cold water inlet temperature T (°C)	Cold water outlet temperature T (°C)
1	0.010	87.1	85.6	27	34.3
2	0.010	84.3	74.3	27	33.1
3	0.010	70.9	62.8	27	31.7
4	0.006	87.4	80.1	27	32.1
5	0.006	84.8	66.2	27	31.3
6	0.006	70	58	27	30.6

The experimental results of the heat exchanger with porous (WP) wire screens show that when the hot air inlet temperature of 87.1 °C flows through the outer pipe at a mass flow rate of 0.010 kg/s, heat transfer from hot air to cold water occurs, causing the cold water outlet temperature increase to 7.3 °C (tab. 4). As illustrated in Figure 6a, numerical modeling indicates that the cold water exit temperature increases to 6.05 °C when the hot air input temperature is specified at 87 °C and the mass flow rate is set at 0.010 kg/s. The numerical results and experimental outcomes are comparable. The heat exchanger without porous (WOP) wire screens experimental data show that when the hot air input temperature of 87.4 °C passes through the outer pipe at a mass flow rate of 0.010 kg/s, the cold water outlet temperature increases to 4.7 °C (tab. 3). Numerical modeling shows that when the hot air input

temperature is specified at 87 °C and the mass flow rate is set at 0.010 kg/s, the cold water exit temperature rises to 3.14 °C, as shown in Figure 6d. Similarly, as shown in tab. 3 and tab. 4, satisfactory experimental and numerical findings are obtained for both scenarios (WP & WOP) when the hot air mass flow rate is adjusted to 0.006 kg/s. The results show a reasonably equal relationship between the experimental validation and the numerical research outcomes.

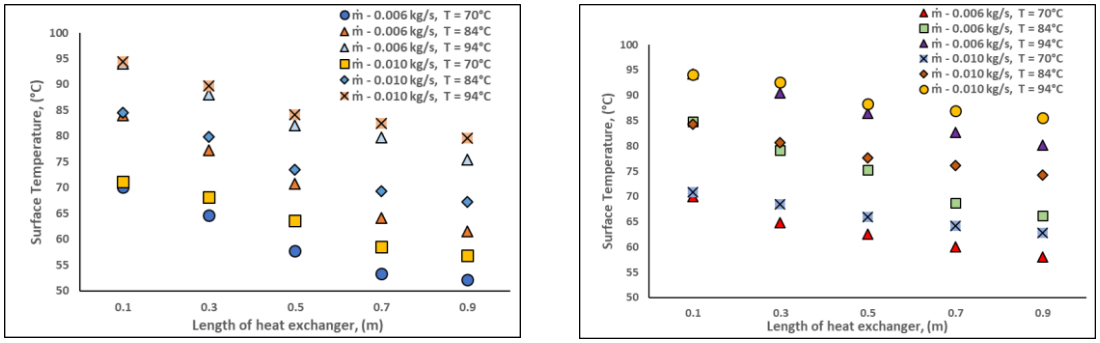

(a) (b)

Figure 7. Surface temperature distribution along outer pipe, (a) without porous, (b) with porous

Fig. 7 illustrates that the surface temperature decreases with axial distance along outer pipe due to heat transfer from hot air to cold water in this counter flow heat exchanger. As a function of heat exchanger length and hot air mass flow rate, it also displays the observed temperature distributions of the outer pipe surface for both with porous (WP)screens and without porous (WOP) screens. The experimental findings are obtained with two different mass flow rates and three different hot air input temperatures. Also,fig. 7 shows the hot air temperature distribution of the porous heat exchanger, which showed a higher surface temperature distribution than the non-porous hot air temperature distribution for constant hot air intake

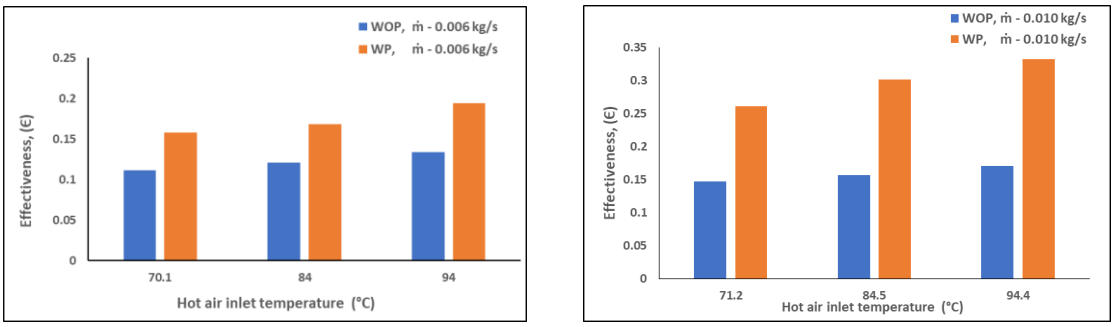

(a) (b)

Figure 8. Variations of hot air inlet temperature to effectiveness for without porous (WOP) and with porous (WP) heat exchangers, (a) ṁ - 0.006 kg/s, (b) ṁ - 0.010 kg/s.

The heat exchanger's effectiveness shown in fig. 8 for two distinct mass flow rates (0.010208 kg/s and 0.006125 kg/s) and three different hot air input temperatures (70°C, 84°C, and 94°C). It is clear that heat exchangers using porous materials are greater in effectiveness than those without porous heat exchangers. Fig. 9a demonstrates that at three different hot air input temperatures (70°C, 84°C, and 94°C) and a mass flow rate of 0.006125 kg/s, a heat exchanger with porous (WP) provides a higher NTU and effectiveness compared to a heat exchanger without porous (WOP).

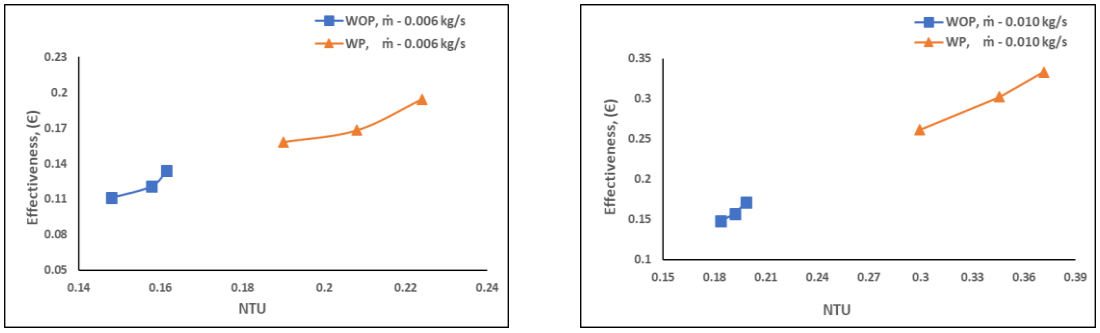

(a) (b)

Figure 9. Realtion between NTU to effectiveness for without porous (WOP) and with porous (WP) heat exchangers, (a) ṁ - 0.006 kg/s, (b) ṁ - 0.010 kg/s,

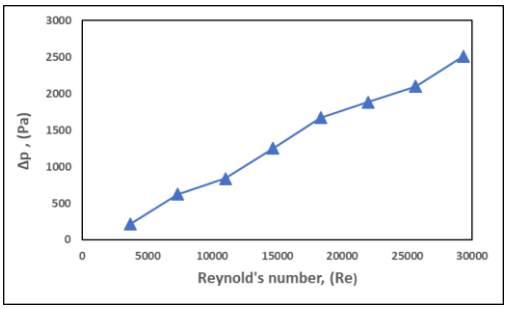

Figure 10. Relation between pressure drop to hot air Reynold's number on heat exchanger with porous wire screens

Similarly, fig. 9b indicates a porous heat exchanger (WP) offers a greater NTU and effectiveness at a mass flow rate of 0.010208 kg/s. On a heat exchanger with porous wire screens, fig. 10 shows the link between hot air Reynold's number and pressure drop. An increase in mass flow rate of hot air causes the Reynold's number rises, which raises the pressure drop.

5. Conclusion

The goal of the research was to improve heat transfer in counterflow heat exchangers by adding metallic wire screens to the inside of the outer pipe. The numerical modelling of porous heat exchanger testing on stainless steel wire screens was done using Ansys (Fluent). This study assessed the performance of the porous heat exchanger. The results of the experimental validation and numerical studies are extremely comparable.

The following conclusions were gathered from the discussion of the results:

a) The effectiveness of a porous heat exchanger rises from 0.17 to 0.33 when compared to one without porous material.
b) Furthermore, compared to a heat exchanger without porous material, the NTU of a porous heat exchanger increases from 0.198 to 0.372.
c) The surface temperature drops with axial distance due to heat transfer from hot air to cool water. As the mass flow rate of hot air increased steadily, it also raised the surface temperature.
d) Effectiveness increases along with NTU.

Nomenclature

d :Wire diameter (m)
d_h : Hydraulic diameter (m)
K :Permeability of the wire screen (m^2)
P :Pressure (Pa)
Re :Reynolds number
v_i : Fluid velocity through the pores (m s^{-1})
x : Screen thickness (m)
ε : Porosity
μ : Dynamic viscosity (Pa s)
ρ : Density (kg m^{-3})
Q_c : Heat transfer rate of cold fluid (W)
Q_h : Heat transfer rate of hot fluid (W)
Q_{act} :Actual heat transfer rate (W)

References

[1] Brundret, E., Prediction of Pressure Drop for Incompressible Flow Through Screens, *Journal of Fluids Engineering*, 115 (1993), pp. 239-242
[2] Bogdan, I, Pavel., Abdulmajeed, A, Mohamad., An Experimental And Numerical Study On Heat Transfer Enhancement For Gas Heat Exchangers Fitted With Porous Media, *International Journal of Heat and Mass Transfer*, 47 (2004), pp. 4939–4952
[3] Chen Shuangtao., *et al.*, A Numerical Model Of Thermal Analysis For Woven Wire Screen Matrix Heat Exchanger, *Cryogenics*, 49 (2009), pp. 482–489
[4] Yadav, J,P., Bharat Raj Singh., Experimental Set up of Air Conditioning System in Automobile Using Exhaust Energy, *All India Seminar on Sources of Planet Energy, Environmental & Disaster Science: Challenges and Strategies (SPEEDS-2013)*, 5 (2013), pp. 71-80
[5] Wael, I, A, Aly., *et al.*, Thermal Performance Of A Diffusion Absorption Refrigeration System Driven By Waste Heat From Diesel Engine Exhaust Gases, *Applied Thermal Engineering*, 114 (2017), pp. 621–630
[6] Peng, Y,B., *et al.*, Experimental Study On The Influence Of Wire Diameter On The Internal Flow Behaviour Of Woven Metal Screens, *IOP Conf. Series: Materials Science and Engineering*, 164 (2017) 012003, pp. 1-8
[7] Edgar Avalos Gauna., Yuyuan Zhao., Numerical Simulation of Heat Transfer in Porous Metals for Cooling Applications, *Metallurgical And Materials Transactions B*, 48B (2017), pp. 1925-1932
[8] Isbeyeh, W, Maid., *et al.*, Experimental Study Of Heat Transfer Enhancement In Heat Exchanger Using Porous Media, *Global Journal of Engineering Science and Research Managemen*t, 4 (2017), pp. 82-91
[9] Hannes Fugmann., *et al.*, Wire Structure Heat Exchangers New Designs for Efficient Heat Transfer, *Energies*, 10, (2017), 1341, pp. 1-17
[10] Nikolai Chernov., Heat Exchangers Of Increased Thermal Efficiency For Power And Technological Machines: Development And Research, *MATEC Web of Conferences*, 212 (2018), 01034, pp. 1-15
[11] Patrick, N, Okolo., *et al.*, Numerical Assessment Of Flow Control Capabilities Of Three Dimensional Woven Wire Mesh Screens, *European Journal of Mechanics / B Fluids*, 76 (2019), pp. 259–271
[12] Srinivasan, K, V., *et al.*, Design And Development Of Porous Regenerator For Stirling Cryocooler Using Additive Manufacturing, *Thermal Science and Engineering Progress*,11 (2019), pp.195–203
[13] Mukul Kumar., Randip Kumar Das., Experimental Analysis Of Absorption Refrigeration System Driven By Waste Heat Of Diesel Engine Exhaust, *Thermal Science*, 23 (2019), 1, pp. 149-157
[14] Siddhartha Yadav, J., *et al.*, A Novel Development of Vapor Absorption Air-Conditioning System using Engine Exhaust Heat, *Research and Applications of Thermal Engineering*,3(2020),3, pp.1-5
[15] Sayed, M, A., *et al.*, Performance Evaluation Of Wire Mesh Heat Exchangers, *Applied Thermal Engineering*, 169 (2020), 114891, pp. 1-9
[16] Salem Alabd Mohamed., Munawar Nawab Karimi., Analysis and Optimization Of Vapor Absorption Generator-heat Exchanger using Kern Method and CFD, *Journal of Thermal Engineering*, 6 (2020), 4, pp. 440-459

[17] Isbeyeh, W, Maid., *et al.,* Numerical Analysis For Enhancing Transferred Heat In Porous Counter Flow Heat Exchanger, *IOP Conf. Series: Materials Science and Engineering*, 745 (2020), 012081, pp. 1-12
[18] Xiang-Bo Feng., *et al.,* Numerical Simulations Of Convection Heat Transfer In Porous Media Using A Cascaded Lattice Boltzmann Method, *International Journal of Heat and Mass Transfer*, 151 (2020), 119410, pp. 1-10
[19] Andres Zapata., *et al.,* CFD Modelling Of The Ammonia Vapour Absorption In A Tubular Bubble Absorber With NH3/Lino3, *Case Studies in Thermal Engineering*, 27 (2021) ,101311, pp. 1-13
[20] Trilok, G., *et al.,* Correlations and Numerical Modeling of Stacked Woven Wire-Mesh Porous Media for Heat Exchange Applications, *Energies*, 15 (2022), 2371, pp. 1-25.
[21] Le Xuan Hoang Khoa., *et al.,* Numerical Simulation of Solid and Porous Fins' Impact on Heat Transfer Performance in a Differentially Heated Chamber, *Mathematics*, 10 (2022), 263, pp. 1-14
[22] Hassan, O, H., *et al.,* Investigation Of Heat Transfer And Pressure Drop In A Porous Media With Internal Heat Generation, *Case Studies in Thermal Engineering*, 32 (2022), 101849, pp. 1-13
[23] Saad, S, Alrwashdeh., *et al.,* The Effect of Heat Exchanger Design on Heat transfer Rate and Temperature Distribution, *Emerging Science Journal*, 6 (2022), 1, pp.128-137
[24] Ghanim, M, Algwauish., *et al.,* A Numerical Simulation of Convection and Conduction Heat Transfer for a Fluid in a Porous Medium, *European Journal of Pure and Applied Mathematics*, 16 (2024), 2, pp. 833 – 846
[25] Eman Mohamed Ismail., *et al.,* Heat Exchanger Design and Optimization for Industrial Applications, *Nanotechnology Perceptions*, 20(2024), S3, pp. 211–229
[26] Zengliang Chen., *et al.,* Optimization Design and Performance Study of a Heat Exchanger for an Oil and Gas Recovery System in an Oil Depot, *Energies*, 17 (2024), 2631, pp.1-18
[27] Jiangtao Chen., *et al.,* Parameter Optimization of an Absorption Heat Exchanger with Large Temperature Difference, *Processes*, 12 (2024), 1669, pp.1-14

Submitted: 03.07.2025
Revised: 10.09.2025
Accepted: 16.09.2025